ГОДИШНИК на Минно-геоложкия университет "Св. Иван Рилски", Том 48, Св. III, Механизация, електрификация и автоматизация на мините, 2005
ANNUAL of the University of Mining and Geology "St. Ivan Rilski", Vol. 48, Part III, Mechanization, electrification and automation in mines, 2005

THE AMELIORATION OF THE NON-UNIFORM LOAD DISTRIBUTION IN SHOULDERED THREADED CONNECTIONS USED FOR THE LARGE DIAMETER DRILL STEM

Adrian Creitaru[1], Alexandru Pupazescu[2]

[1,2] *Petroleum-Gas University, Ploiesti, Romania*

ABSTRACT: One of the most commonly employed connections for large diameter drill stem components is the shouldered threaded one. Due to high axial and torsional load, these joints can use a special asymmetric thread. For this type, the stress and deformation states are revealed using the Finite Element Method. As acknowledged, the load distribution over the spires is non-uniform. Consequently, it causes the development of high stress areas in the proximity of the shoulder. The overloaded state of the first spire engaged is obvious. Therefore, the root of its active flank becomes a hard stress concentrator. The present paper proposes a method for the overload state amelioration by using the fine pitch adjustment. It can be made of some of the spires near the shoulder, at the pin of the joint. As a result of the FEM application, the stress maps obtained show the maximum level in a certain ameliorated situation. The paper also determines the optimal pitch adjustment proper to a determined load state.

ПОДОБРЯВАНЕ РАЗДЕЛЯНЕТО НА НЕЕДНОРОДНИЯ ТОВАР ЧРЕЗ ВРЪЗКИ, ИЗПОЛЗВАНИ ПРИ БУРГИЯ С ГОЛЯМ ДИАМЕТЪР

Адриан Крейтару[1], Александру Пупазеску[2]
[1,2]Университет за нефт и газ, Плоести, Румъния

РЕЗЮМЕ. Една от най-натоварваните връзки при употребата на бургията с голям диаметър е раменната. Във връзка с голямото аксиално и торзиално натоварване, тези връзки могат да използуват специални асиметричен нишки. При този вид свързвания, състоянията на напрежение и деформация се определят чрез използуване на Метода на крайния елемент (FEM). Тъй като е прието, че разпределението на товара над шпицовете (спиралата) не е еднородно, то това причинява образуването на зони с голямо натиск на местата близо до рамото. При първото натоварване, претоварената зона е очевидна. Поради това в дъното на неговият активен фланг настъпва концентрация на високо напрежение Настоящата статия предлага метод за облекчаване на претоварените зони, чрез използване на фина настройка. Това може да бъде направено на няколко пружини близо до рамото, при мястото на съединението. Като следствие от приложението на FEM, напрежение, което се получава показва максималното ниво в определено облекчено положение. В статията също така са определени подходящи нива на натоварване за даден товар.

1. General outlook

1.1. Large Diameter Rotary Blind Drilling

The large diameter Rotary blind drilling uses a similar method of oil & gas drill practice.

Though performing methods are similar, the characteristics of the big hole are different. The depth of the hole is, generally, in the 200…600 *m* domain (in seldom cases, up to 1000 *m*, or more) and the nominal diameter goes to 2,5…6 *m* (Creitaru, 2004; Iordache, 1983).

The stem structure is similar to the conventional drilling but the overall dimensions and weight of the components (those which determine high level loads strain and stress) should be mentioned.

The drill unit has the same functions as usual for the drill stem movement: the rotary and thrust of the rock bit. The sludge (and liquid or compressed air, if necessary) circulation determines the structure and type of pipes. In any case, the drill pipe joints can be used under one of following three forms:

- *threaded shouldered connections;*
- *flanged connections;*
- *bayonet connections.*

As known, the threaded and the flanged connections are the most frequently used. This paper refers only to the threaded joints.

The threaded conical shouldered connections, used in large diameter drilling, have specific geometry (Iordache, 1983). It refers to the asymmetry of the thread profile, which is obviously different by the API well known symmetrical profile.

The stem building is similar to the petroleum activity, by adding successive pipes to the tubular structure. Each make of the threaded joint requires the pre-load torque (M_{ts}).

Last studies on pre-load torque (Creitaru, 2002; Creitaru, 2004) recommend, as a possible solution, the differential torque choice.

That means to calculate and apply – for each k=(1…n) joints the specific $M_{ts}^{(k)}$ values, that involve specific and gradual axial pre-load, $F_o^{(k)}$, for each of them. The stem structure, general load and each joint (connection) load are shown in figure 1.

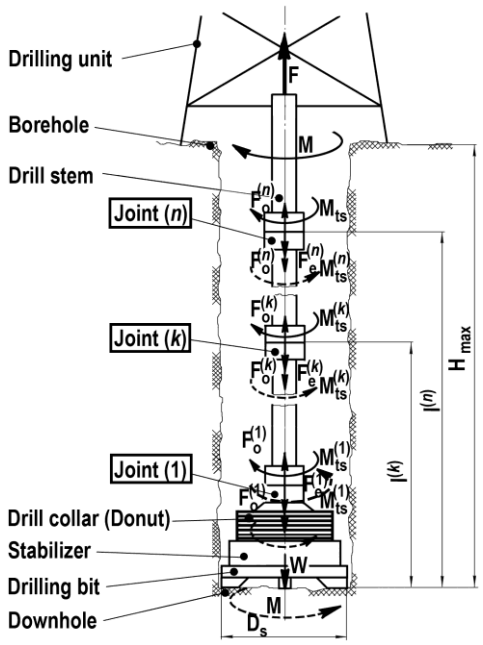

Fig. 1. The general stem structure and load; each joint (1 – *n*) load

1.2. The loaded condition of the stem connections

The differential torque, if positional numbering is from (*1*) – up to the drill collars to (*n*) – at the mouth of the bore are in following relation (Creitaru, 2004):

$$M_{ts}^{(1)} < M_{ts}^{(2)} < \ldots < M_{ts}^{(k)} < \ldots < M_{ts}^{(n)} \tag{1}$$

The equation above determines a similar axial pre-load distribution, at the make joints moment:

$$F_o^{(1)} < F_o^{(2)} < \ldots < F_o^{(k)} < \ldots < F_o^{(n)} \tag{2}$$

Figure 2 shows the overall axial load for the "Joint k" (*a*) and the conventional "load-deformation" diagram (*b*).

After the initiation of pipes' connections (fig. 2., *b*, line 1), stem section made is a running tool into the well. This moment, the axial load of each connection is changing: every component has its own resultant of all forces (fig. 2., *b*, line 2).

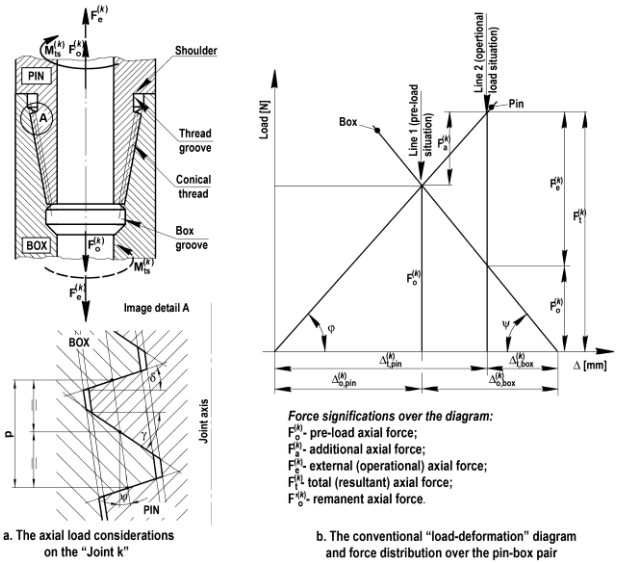

a. The axial load considerations on the "Joint k"

b. The conventional "load-deformation" diagram and force distribution over the pin-box pair

Fig. 2. The overall axial load for the "Joint k" (*a*) and the conventional "load-deformation" diagram (*b*).

The load-deformation diagram shows the different strain of both components, in the several two situations:

- when the *pin* and *box* components are made-up; the $M_{ts}^{(k)}$ application – for each (*k*) joint – involves different axial pre-loads, $F_o^{(k)}$, that determines axial tension for the pin and axial compression for the box; the mechanical phenomena is described by the line 1 (fig. 2.1., *b*);
- when pipes are running into the well, the resultant load for the joint is defined by the line 2 of the diagram (fig. 2.1., *b*); the pin is overloaded cause the external (operational) force, $F_e^{(k)}$ - equivalent of the bottom resultant weight; the total (resultant) axial tension for the pin becomes $F_t^{(k)}$; the box load situation is also changed this case; the axial compression decreases at the $F_o^{'(k)}$ level.

The intercourse for these forces (as related axial loads) is well known as the load-deformation theory.

When operational axial forces $F_e^{(k)}$ become known using the weight cumulative calculus, the remnant axial forces can be determined by the equation:

$$F_o^{'(k)} = (0{,}25 \ldots 0{,}5) \cdot F_e^{(k)} \tag{3}$$

Equation (3) offers certain comments because the remnant force – required for the seal condition on shoulders – can be substantially reduced, in case of airlift internal circulation; this case, the remnant axial force could be recommended:

$$F_o^{'(k)} = (0{,}15 \ldots 0{,}4) \cdot F_e^{(k)} \tag{3'}$$

In consequence, the resultant (total) axial load – needed for the pin dimensioning – becomes:

$$F_t^{(k)} = F_e^{(k)} + F_o^{'(k)} \tag{4}$$

The determination of the additional force easy comes from the reflexive relation:

$$F_a^{(k)} = k_o \cdot F_e^{(k)} \tag{5}$$

where k_o is the load factor, which depends on the complex geometry of pin and box by the rigidity factors, c_p (for pin) and c_b (for box). Usual values determined by calculus for the load factor (k_o) are a bit higher than 0,4 (Creitaru, 2004).

This force determination goes to the axial pre-load, which is necessary for the make-up torques, at each (*k*) level of connections. True to the pattern described in the figure 2, the axial pre-loads are:

$$F_o^{(k)} = F_t^{(k)} + F_a^{'(k)} \tag{6}$$

Than, the determination of the make-up torques, $M_{ts}^{(k)}$ – for the connections (1-*n*) – are as following:

$$M_{ts}^{(k)} = M_{f,th} + M_{f,sh} = a_s \cdot F_o^{(k)} \tag{7}$$

where:

- $M_{f,th}$ is the frictional torque, specific for the threaded zone;
- $M_{f,sh}$ is the frictional torque, specific for the shoulder:
- a_s *is the make-up factor, that can be express by the following equation:*

$$a_S = \frac{d_{2,m}}{2} \cdot \mathrm{tg}\left(\beta_m + \varphi'\right) + \frac{\mu_{sh}}{3} \cdot \frac{d_{e,sh}^3 - d_{i,sh}^3}{d_{e,sh}^2 - d_{i,sh}^2} \qquad (8)$$

The operands in equation (8) are the acknowledged ones: $d_{2,m}$ is the thread diameter for the measurement plane; $d_{e,sh}$ and $d_{i,sh}$ are the external and internal limits of the shoulder; β_m is the incline of the thread spire; φ' is the friction ratio ($\varphi' = \mathrm{arctg}(\mu_{th} / \cos\delta)$) and μ_{sh} is the friction factor for the shoulder of the joint.

2. The Finite Element Method analysis of the threaded shouldered connection

2.1. The main research objectives

The Finite Element Method (MEF) is one of the most useful methods in the structure design.

Its aim is to determine a complex state of stress and strain and to emphasize the load distribution on spires of its thread. This paper is a part of an ample research plan, using a part of technical results (Creitaru, 2004).

The main research directions were following:

- to determinate the state of stress and strain for the threaded shouldered connections used for the large diameter drill stem;
- to analyse and optimize the special asymmetrical thread in use;
- to determine the main concentrators effects;
- to analyse the conditions for using the multiple thread for this kind of connections.

For these purposes, the object of modeling and analyse is one of the most used shouldered connection for large diameter stem assembly: the 14 $^3/_8$ *inch* size.

Last years, FEM applications on threaded connections were developed in many countries, in similar directions (Marx, 2001).

2.2. The program, modeling and structural results

For the MEF applications, as well known, there are a lot of programs to use. The 5.6 version of ANSYS program leads to good analyse results.

The model created had to include both the components of the joint: the pin and the box. The model included only the target zone of the assembly, in the shoulder's neighborhood.

Thus, strategic reasons of research determine the option for the parametric initialization of the thread; it gives the possibility of varying the geometrical elements (in successive runs): conicity, active and passive flank angles, pitch and others.

The 2D axis-symmetric model uses a number of 8696 elements (Plane 2) for this ANSYS application. The final result of the connection modelling is shown in the table 1.

Table 1.
The characteristics of the model of the joint

The type of axis-symmetric elements used for model	**PLANE 2**, elements with **6** nodes, **2D** type
The total number of elements	**8696** elements
The total number of nodes	**17.722** nodes
The type and the number of contact elements	Contact pairs (for surface) **TARGE 169** and **CONTA 172** (for μ = 0,08)

For the composed model we used generated points (that

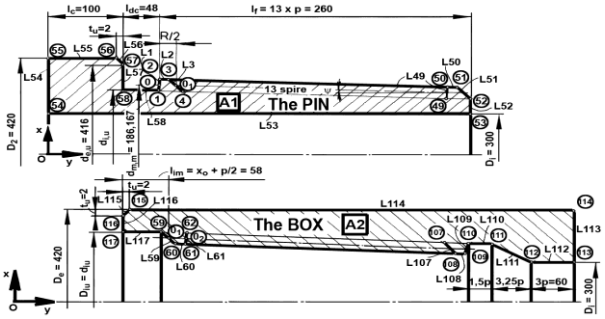

become nodes), lines and areas and, finally, volumes.

Fig. 3. The pin and box model, generated to use in ANSYS program

Figure 3 presents the model generated in this structure (both pin and box elements present).

The modeling also considers the *real configurations* that belong to the elements: the real roots at the base of the active and passive flank, the grooves of the threaded pin and box, the double tapering of the spires etc.

The increments in use have different sizes, thicker in the zones of maximum interest: flank roots, grooves, shoulder.

2.3. The load models applied in ANSYS

If the purposes we have in view by MEF method are the analysis of stress and deformations – in the pre-load and external strain conditions – the model has to reproduce real situations. In consequence, we must choose such load cases.

The cases to consider are based on the scheme reproduced in the figure 4.

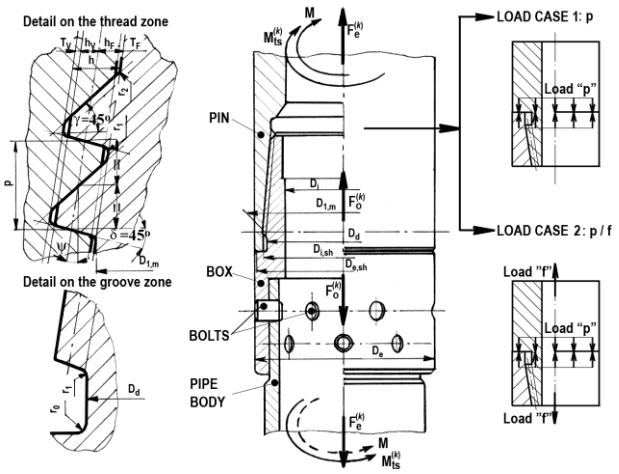

Fig. 4. Dimensional structure of connection, thread type and load cases

The values of the load were considered the heaviest in strain connection – which is the "*n*" joint (situated at the mouth of the hole.

The pre-load cases are synthetically detailed in the table 2. It shows the real load in practice, equivalency, and the way to simulate it by program, symbol, and practical values in use.

Table 2
Pre-loads considered in the FEM application

Real load symbol	Values used [kNm]	Equiv. load symbol	Values used [kN]	Type strain model	**Symbol**
$M_{ts}^{(n)}$	39	$F_o^{(n)}$	1125	Press.	**p50**
	78		2251	Press.	**p100**
	117		3376	Press.	**p150**

This pre-load modelling *LOAD CASE 1* shows the influence of the make-up torque (and axial pre-load force involvement) to the stress and deformation state in all connections.

The influence of combined case of *LOAD CASE 2* shows what happens when the pipes are running into the well, when resultant axial load strains the joint (*n*). This cases are synthetically detailed in the table 3.

Table 3
Combined loads considered in the FEM application

Real load symbol	$M_{ts}^{(n)}$ values used [kNm]	$F_o^{(n)}$ values used [kN]	$F_e^{(n)}$ values used [kN]	Type strain model	**Symbol**
$M_{ts}^{(n)}$ and $F_e^{(n)}$	39	1125	1360	Press.	**p50/f20**
			3400	Press.	**p50/f50**
	78	2251	1360	Press.	**p100/f20**
			3400	Press.	**p100/f50**
	117	3376	1360	Press.	**p150/f20**
			3400	Press.	**p150/f50**

2.4. Results of the FEM analysis

The results obtained by running the ANSYS application are comprised of a list of the stress and deformations – which were selected for the nodes situated on the contour – and of the axial, radial, circumferential and von Mises stress maps.

The maps were selected in two variants: for all the pin-box structure (fig. 5) – which shows the stress level all over the joint – and details-map – to concentrate only on high stress zones of interest (fig. 6).

The samples of graphic results are selected to show the general distribution of stress (σ_y, σ_x, σ_z and σ_{ech} – von Mises). Figure 5 can be used to identify the high stress zones and have a global evaluation.

Figure 6 presents samples of detailed maps. These were determined for the combined loads (*LOAD CASE 2*), for the strain symbolised **p100/f20**. Theses maps show more details on stress disposed in zones of high levels – the pin groove and roots of the first spires near the shoulder. However, this is the zone of maximum stress in analyse.

3. The improvement of the load distribution over the threaded shouldered connections

3.1. Preliminary useful deductions as FEM analysis output

The FEM analysis brings some useful conclusions regarding the threaded shouldered connections (Creitaru, 2004):

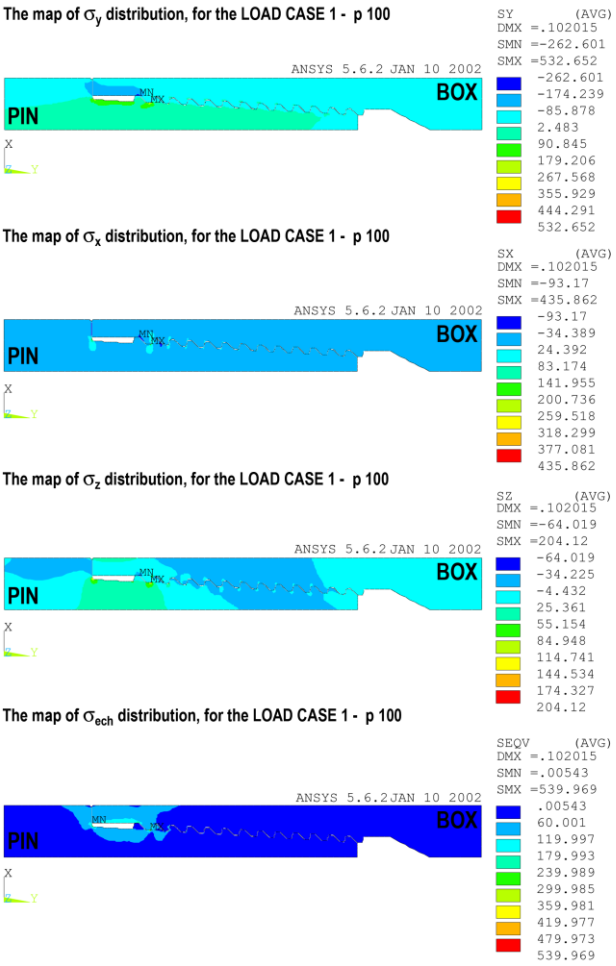

Fig. 5. Picked sample of stress maps, determined for the load p100

- the pin-box pair model shows that the higher stress level always belongs to pin's threaded zone;
- the global stress state, in both pin and box components, is, generally, at a moderate low level; the high stress zones are restricted locally;
- both pin and box components shows that the highest level belongs to the threaded and groove zones; the active flank roots areas of the pin points out the highest stress levels, cause of the strongest stress concentrator, that is, the thread (Marx, 2001);
- the stress analysis shows a non-uniform load distribution on thread spires, from shoulder to the bit of the conical pin;
- both load cases in analyse – pre-load and combined axial load – shows that the stress level is higher on first 3-4 helical spires of the pin;
- the maximum stress point – all load cases, both strength variants – is always situated at the second spire basis (root of the active flank), which is the first spire in load engagement;
- as expected, the combined strength (*LOAD CASE 2*) always determines higher stress levels;
- as expected, the weight of axial stress (σ_y), reported to equivalent stress (σ_{ech}), is always higher; by contrast, radial (σ_x) and circumferential stress (σ_z) levels are much lower.

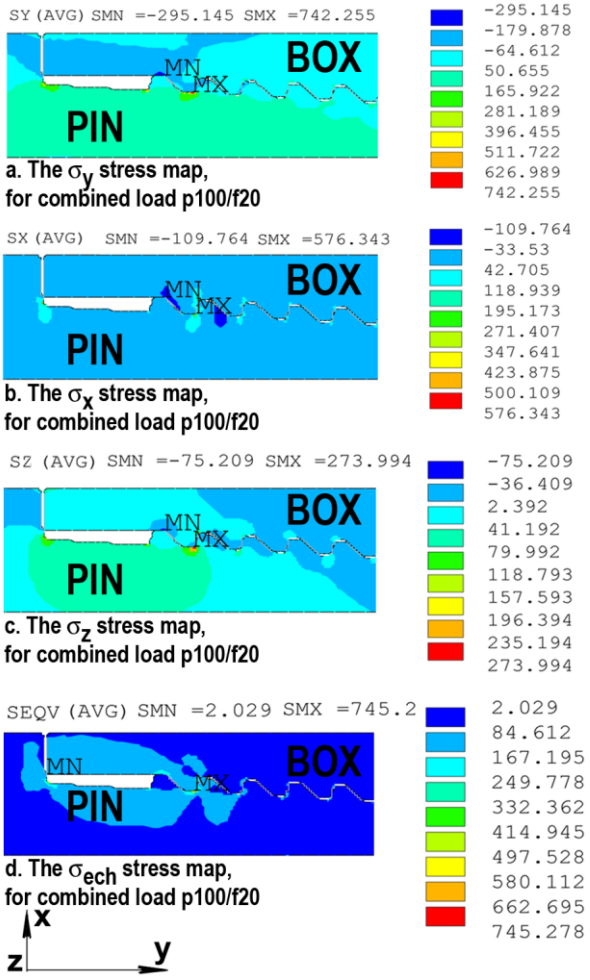

Fig. 6. Picked sample of stress maps, determined for the combined load p100/f20

3.2. The load distribution over the thread of pin and box

As presented before, the load distribution along the 13 helical spires of the thread is non-uniform.

The FEM analysis (Creitaru, 2002; Creitaru, 2004) conducted to the load distribution draw out. Figure 7 presents, as an instance, the load distributions for some of the cases analysed.

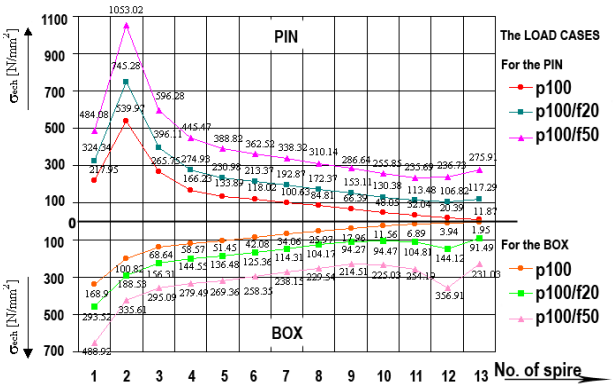

Fig. 7. The non-uniform load distribution over the spires of pin and box

It's plainly obvious that non-uniformity of load distributions is an undesirable consequence and this makes necessary to adopt measures to equalize it.

3.3. The pitch adjustment description

The pitch adjustment of the conical thread of the joint refers to a fine (and accurate) profile modification.

It can be operated to the pin or box component, but pin processing is more simply.

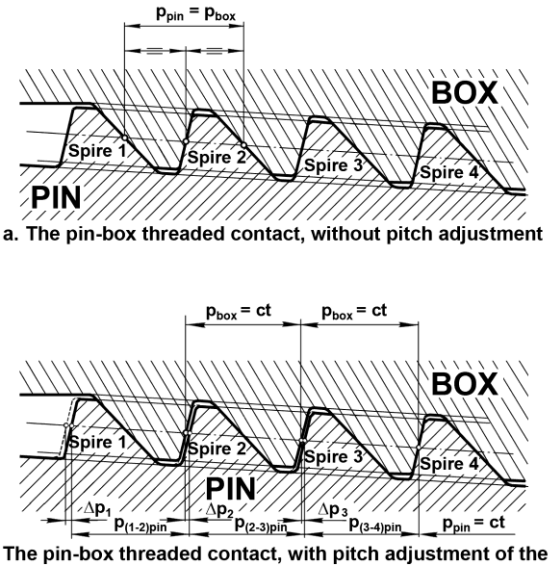

Fig 8. The pin-box contact, on usual and pitch adjusted connection

The pitch adjustment means helical cut of the active flank, executed on first 2-4 spires from the shoulder. The cutting depth has to be gradual, decreasing from the first helical spire, up to the 3-rd, or to the 4-th spire, in nullification.

This pitch gradual adjustment modifies the initial contact of pin and box thread, creating a local clearance. This clearance between similar spires of pin and box are thinner from the first

spire-pair of the shoulder to the last pair (3-rd or 4-th), where this clearance is finely annulled.

This decreasing clearance determines that, initially, when make-up torque is not yet applied, the flanks contact on "higher load spires" doesn't initially exist.

Afterwards, when pre-load comes, the elastic deformations of elements modify the clearance and the re-distribution of the load appears.

The pitch modification, $\Delta p_{(i-j)}$, is decreasing, from the first pin-box pair of spires. Figure 8 shows the graphic disposal of the spires, on this area of interest.

3.4. The pitch adjustment settling

Evidently, the adjustment settle is both difficult and necessary. A suggestive method to estimate the length of pitch adjustment is by analysing the behaviour of pin deformations, along the first 3-4 spires.

For this evaluation, the FEM displacement results are the best option.

In this analysis, three different levels of pitch adjustment were settled, for both load cases (*LOAD CASE 1* – **p100** and *LOAD CASE 2* – **p100/f20**):

- the **low level adjustment** (**s1**), Δp=0,01 *mm*; this case:
  - spires 4…13 have normal thread;
  - spire 3 has Δp=0,01 *mm*;
  - spire 2 has Δp=0,02 *mm*;
  - spire 1 has Δp=0,03 *mm*;
- the **medium level adjustment** (**s2**), Δp=0,02 *mm*; this case:
  - spires 4…13 have normal thread;
  - spire 3 has Δp=0,02 *mm*;
  - spire 2 has Δp=0,04 *mm*;
  - spire 1 has Δp=0,06 *mm*;
- the **high level adjustment** (**s3**), Δp=0,05 *mm*; this case:
  - spires 4…13 have normal thread;
  - spire 3 has Δp=0,05 *mm*;
  - spire 2 has Δp=0,10 *mm*;
  - spire 1 has Δp=0,15 *mm*.

3.5. The FEM main results and interpretation

The FEM running by ANSYS determined the data list of nodes stress and displacements, and also all types of stress maps ((σ_y, σ_x, σ_z and σ_{ech}). As known, using Huber Henchy-von Mises Theory, equivalent stress expression is calculated:

$$\sigma_{ec} = \sqrt{\sigma_1^2 + \sigma_2^2 + \sigma_3^2 - (\sigma_1\sigma_2 + \sigma_2\sigma_3 + \sigma_3\sigma_1)} \qquad (9)$$

There were selected, for these cases, the stress data nodes by contour, to compare cases (**s1**), (**s2**), (**s3**) and the un-adjustment case of thread.

When connection is in pre-load state (*LOAD CASE 1* **p100)**, the modifications of stress maps (in the interest zone) is shown by the figure 9. There were selected only these cases: (**s1**), (**s3**) and, by opposite, the un-adjusted standard case (**std**).

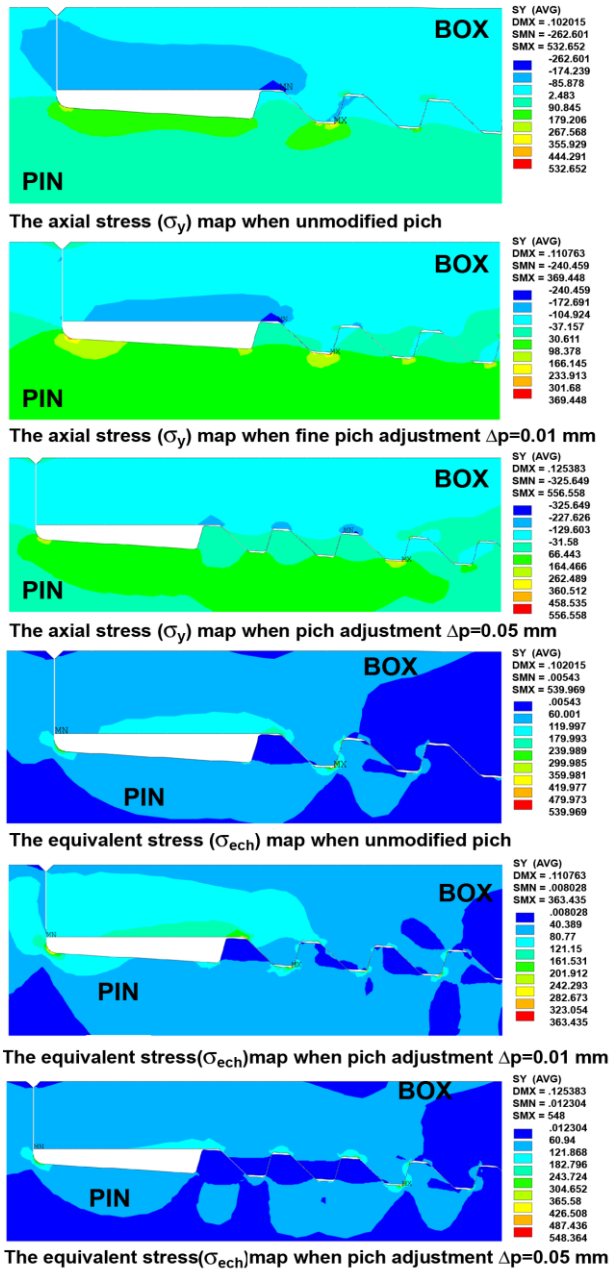

Fig. 9. Comparative stress (σ_y and σ_{ech}) maps for the LOAD CASE 1

These results give a global image of stress level evolution. A better evaluation of pitch adjustment procedure should result by analysing the stress distribution over the 13 spires, for standard (**std**), (**s1**), (**s2**) and (**s3**) situations. Figure 10 presents the stress distributions in these evolution cases. We can emphasize that:

- the(**s1**) case determines a substantial decrease of the maximal stress level on critical spires 2 and 3, beside a high equalization;
- the (**s2**) case determines a temperate decrease of the stress on spires 1-3; the max. loaded spires is transferred from the 2nd to the 4th spire;
- the (**s3**) case determines the transfer of the max. loaded point from 2nd to the 4th spire beside its bit raising level.

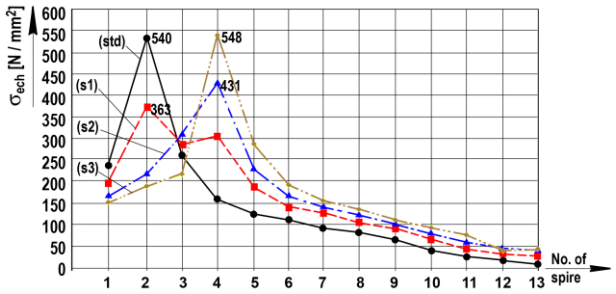

Fig. 10. The stress distribution for standard (std), (s1), (s2) and (s3) situations

The same effect – the attenuation of stress max. values – can be observed in second load case (*LOAD CASE 2* – **p100/f20**) – for the same (**std**), (**s1**), (**s2**) and (**s3**) situations.

The graphic representation of the stress distributions, on the spires of the pin is presented in figure 11.

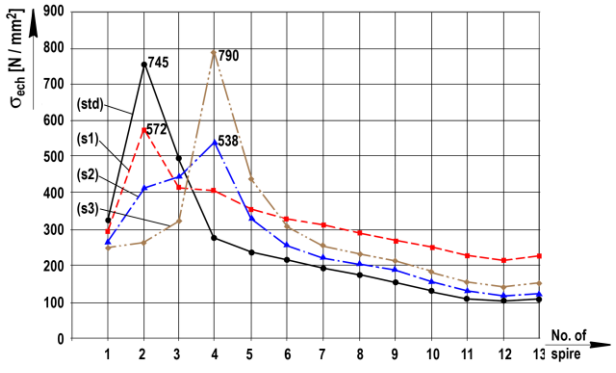

Fig. 11. The stress distribution for standard (std), (s1), (s2) and (s3) situations

Recommended for publication by the Editorial board of
Section "Mechanization, Electrification and Automation in Mine"

4. Conclusions

The FEM analysis on the connections operated by the pitch adjustment of the thread leads to the following conclusions:

- the smaller values of adjustment (<0,01 *mm*) doesn't modify the stress distributions and so, it becomes useless;
- higher values of adjustment (>0,03 or 0,04 *mm*) change only the place of the max. stress development (from 2nd to the 3rd or 4th spire); some cases, the absolute max. value is a little bit higher;
- the most spectacular results are obtained for the level of adjustment in Δp =0,01…0,25 *mm* domain (this size of joint and load level); for any other case, FEM study is needed;
- the reduction of the max. stress level on the structure is, generally, evaluated about 25…55%.

References

Creiţaru A., Pupăzescu Al. 2002. *Shouldered Threaded Connections Calculus through Nummerical Methods*, in *Petroleum and Gas Journal* no. 5 (35), Bucuresti, 84 p. (in Romanian).

Creitaru A. 2004. *Contributions to Large Diameter Drilling Stem Connections Analysis*, PhD Thesis, Petroleum and Gas University of Ploiesti, 479 p. (in Romanian).

Iordache Gh. et al. 1983. *Large Diameter Drilling*, Editura Tehnică, Bucuresti, 366 p. (in Romanian).

Marx C., Teodoriu C., Pupăzescu A., 2001. *A New Method to Determine the Stress Distribution in Conical Shouldering Thread Connections*, DGMK- Tagungsbericht, Erdől, Germany.